Russian Geology and Geophysics © 2020, V.S. Sobolev IGM, Siberian Branch of the RAS
Vol. 61, No. 5–6, pp. 634–649, 2020 *DOI:10.15372/RGG2020144* *Geologiya i Geofizika*

Crystallographic Orientation and Geochemical Features of Mineral Inclusions in Diamonds

N.V. Sobolev[a,b,] ✉, Yu.V. Seryotkin[a,b], A.M. Logvinova[a,b]., A.D. Pavlushin[c], S.S. Ugap'eva[c]

[a] *V.S. Sobolev Institute of Geology and Mineralogy, Siberian Branch of the Russian Academy of Sciences, pr. Akademika Koptyuga 3, Novosibirsk, 630090, Russia*

[b] *Novosibirsk State University, ul. Pirogova 1, Novosibirsk, 630090, Russia*

[c] *Diamond and Precious Metal Geology Institute, Siberian Branch of the Russian Academy of Sciences, pr. Lenina 39, Yakutsk, 677980, Russia*

Received 13 January 2020

Abstract—The orientation of 76 mineral inclusions represented by olivine (25 inclusions), pyrope (13 inclusions), and magnesiochromite (38 inclusions) was measured in 16 diamond samples from the major primary diamond deposits of Yakutia: Mir, Udachnaya, Internatsionalnaya, Aikhal, and Yubileynaya kimberlite pipes. The novelty of the study is that it provides a special purposeful approach to selection of samples containing not only olivine inclusions that have been extensively studied in the most recent years after the publication of the book Carbon in Earth (2013). The present collection accounts for more than 25% of all samples studied across the world and includes the most typical mineral inclusions of the predominant peridotitic paragenesis in almost all known kimberlites. Both this experiment and similar studies conducted by foreign colleagues in 2014–2019 have found no inclusions whose orientation meets the epitaxial criterion. Only single magnesiochromite inclusions in three diamonds demonstrate an orientation close to the regular one. A significant correlation between the carbon isotope composition and the mineral composition of inclusions of peridotitic and eclogitic paragenesis diamonds as well as the lack of a correlation with other properties may be considered one of the geochemical features. However, given the numerous published and proprietary data demonstrating the complex diamond growth history and, in some cases, wide variations in the composition of mineral inclusions in different zones, along with the difference in their morphology, the authors a believe that syngenetic and protogenetic inclusions can coexist in the same diamond. This is also confirmed by the discoveries of diamondiferous peridotite and eclogite xenoliths in kimberlites where diamonds are completely enclosed in garnet or olivine. Of particular note is the constant presence of heavy hydrocarbons (rel.%), from pentane (C_5H_{12}) to hexadecane ($C_{16}H_{34}$), that are predominant in fluid inclusions in kimberlite and placer diamonds as well as in pyrope and olivine of diamondiferous peridotite xenoliths.

Keywords: high and ultrahigh pressures, eclogite, peridotite, olivine, garnet, chromite, diamond, coesite, relative orientation of diamond and inclusions, paragenesis, mineral equilibria, geothermobarometry, inclusion morphology, high-density fluid inclusions

INTRODUCTION

Diamond is the deepest-seated material of the Earth's interior, which is available on the Earth surface because of evacuation by kimberlites and lamproites and also redeposition in placers. Diamond is the main material for assessing the composition of the Earth's interior, including the lithosphere and deeper zones.

The discovery history of diamond deposits within the Siberian Platform originates from a detailed study of the petrology of traps extensively presented in the platform and comparison of its geologic features with those of other platforms of the Earth. One of the most important conclusions of this comparison was the assertion that "the geological map of the South African Platform is very similar to the geological map of the Siberian Platform" (Sobolev, 1936). This comparison provided the basis for a scientific prognosis of the diamond presence of the Siberian Platform (Kjarsgaard et al., 2019), which led, based on long-standing work of a large team of geologists, to the discovery of the Yakutian kimberlite province in 1954. This discovery resulted in very active petrological and mineralogical studies of Siberian kimberlites and their constituent minerals, in particular, diamonds, which stimulated intensification of similar studies of South African kimberlites (Dawson, 1984; Arima et al., 2008).

Investigation of the composition of pyrope inclusions in South African (Meyer and Boyd, 1972; Meyer, 1987) and Yakutian (Sobolev et al., 1969a) diamonds using X-ray microprobes proved, as early as the late 1960s, the unique composition of these inclusions in diamonds from different regions, with a high content an increased impurity (wt.%) of

✉ Corresponding author.
E-mail address: sobolev@igm.nsc.ru (N.V. Sobolev)

Cr_2O_3 impurity (5.85–15.9) and a low CaO content (1.22–3.10). These features distinguished them from all previously studied pyropes from heavy-fraction concentrates and deep-seated kimberlite xenoliths (Sobolev et al., 1969b) and substantiated their attribution to the dunite–harzburgite (clinopyroxene-free) paragenesis (Sobolev et al., 1969a, b). Pyrope containing impurities (wt.%) of Cr_2O_3 (8.20) and CaO (1.93) and associated with magnesiochromite containing about 6.5% Al_2O_3 and more than 60% Cr_2O_3 was found in one of the xenoliths of diamondiferous serpentinite (Sobolev, 1977). The discoveries of xenoliths of diamondiferous serpentinites (Sobolev et al., 1969b) and diamondiferous eclogite (Bobrievich et al., 1959) in Yakutian kimberlites enabled assessing, for the first time, the garnet composition in samples from the deepest-seated diamondiferous rocks, despite the much earlier discovery of diamondiferous eclogite xenolith in kimberlites of South Africa (Bonney, 1899), and substantiating the presence of two main geochemical types of deep-seated upper-mantle substrate, peridotitic and eclogitic, where diamonds crystallize. It was first found that the nitrogen content in diamonds from eclogites does not differ from that in diamonds from the host kimberlite (Sobolev et al., 1966). These geochemical types have been fully confirmed by subsequent long-standing studies and accepted in the classification of deep-seated diamondiferous parageneses in a highly cited review (Shirey et al., 2013). These findings enabled identifying the compositions of diamond potential indicators in kimberlites: high-chromium subcalcic pyropes (Sobolev et al., 1969a; Sobolev, 1977), high-chromium spinels (Sobolev, 1977; Sobolev et al., 2019a), which are real diamond indicators and occur in diamondiferous megacrystalline dunites and harzburgites in contrast to common pyropes and spinelides that are indicators of kimberlites, including nondiamondiferous ones. In addition to kimberlites, pyrope-free spinelides are found in some ultrabasic rocks, occurring in the heavy fraction of concentrates during their disintegration (Sobolev, 1977; Nikolenko et al., 2018; Okrugin et al., 2018; Tychkov et al., 2018).

Crystallographic studies in this work were performed to elucidate the ratio of inclusions and the host diamonds, i.e., the timing when the inclusion appeared in the diamond: The inclusion formed before the diamond and then was captured by it (protogenetic), or the inclusion grew simultaneously with the diamond and was captured by it (syngenetic).

According to E.S. Fedorov, crystallography is not only a specific field of geometry but also manifestation of the fundamental features of the material world, and symmetry is a special property of the material world (Borisov et al., 2020). Mineral inclusions in diamonds are a vivid confirmation of that. Inclusions in diamonds, especially olivine and pyrope ones, can have the most unexpected and bizarre morphology and a distorted external symmetry far from that corresponding related to their crystalline structure. For example, fine polycrystalline olivine inclusions were observed in one of the South African diamonds (Harris, 1968). In one of the diamonds from the Mir pipe, a pyrope inclusion looked like a thin plate very similar to lamellar garnets enclosed in mica (Zyuzin, 1967). Sometimes, highly flattened olivine crystals with a widely developed face are found. These olivine inclusions were first described for South African diamond (Mitchell and Giardini, 1953). A series of pyrope inclusions of diverse morphology was described by Bartoshinskii et al. (1980). Important results were obtained in studying the relative orientation of diamond and diamond-hosted olivine (Futergendler and Frank-Kamenetskii, 1961, 1964; Frank-Kamenetskii, 1964). Orlov (1977) summarized the research results and concluded that all materials on the investigation of garnet, olivine, and spinelide inclusions in diamonds, which was performed in the 1960s, indicate that these minerals crystallized simultaneously with diamond and may be considered syngenetic inclusions.

When studying a representative collection of diamonds with inclusions from the Mir kimberlite pipe, we first discovered a type of mineral inclusions, which had not previously been reported in any publication (Orlov, 1959; Harris, 1968), with the faceting of a negative diamond crystal (Sobolev et al., 1970, 1972). On macroscopic examination, the faces of many mineral inclusions can be seen through the octahedral diamond faces and look as triangles strictly parallel to each diamond face.

A pyrope inclusion with dominant sharp-edged octahedral faces was first extracted from diamond and then studied using a goniometer, along with an olivine inclusion (Fig. 1) displaying its own faceting with rounded edges, which complicated these studies (Sobolev et al., 1970).

An industrial quality diamond was an almost isometric octahedron about 8 mm across and 4.25 carats in weight. The olivine crystal (Fig. 1*A*) was noticeably elongated along [001], and its dimensions were 0.25x0.14x0.18 mm. The central parts of vertical zone faces were smooth and flat, and the peripheral ones were rounded.

The garnet inclusion is a faceted crystal of an octahedral habit, 0.30 × 0.19 × 0.17 mm in size, greatly elongated (Fig. 1*B*). Due to distortions, rather long smoothly rounded false edges occurred in the place of octahedron vertices. The equally-sized octahedron faces dominated the crystal and

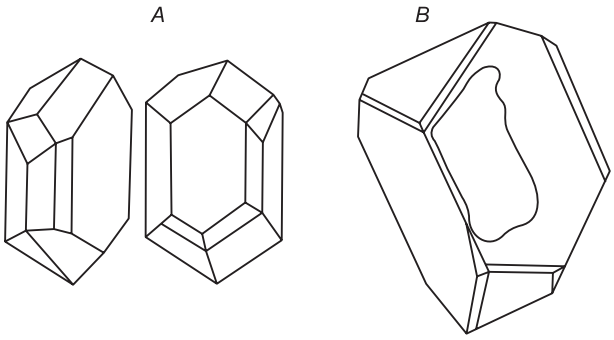

Fig. 1. Olivine (*A*) and pyrope (*B*) crystals extracted from a diamond from the Udachnaya pipe, sample 57/9 (Sobolev et al., 1970).

gave very bright and clear signals on a goniometer. A large lamellar overgrowth was present on one of the faces.

A series of inclusions of olivine, pyrope, chrome diopside, and enstatite monocrystals as well as polymineralic inclusions of these minerals also with an octahedral faceting were reported in (Sobolev et al., 1972). This faceting was not typical of olivine, which is a common diamond inclusion. Along with mono- and polymineralic inclusions with an octahedral faceting, olivines with their own faceting were found in several diamonds. Following these publications, a detailed paper was published, which described similar features of inclusions in diamonds from deposits in South Africa (Prinz et al., 1975). Similar inclusions, in particular pyrope, were found in diamonds from lamproites of Australia (Hall and Smith, 1984).

Subsequent studies of collections of domestic diamonds with inclusions continued identification of inclusions with clear induction relationships with diamond in the case of rutile (Sobolev et al., 1999; Sobolev and Yefimova, 2000; Schmitt et al., 2019) and various morphologies of coesite inclusions, including sharp-edged octahedra (Sobolev et al., 1999). The octahedral faceting imposed by diamond, parallel to its growth zonation, was found in nanoscale olivine inclusions in diamond (Hwang et al., 2018) as well as in many nanoscale high-density fluid inclusions (Logvinova et al., 2008, 2011), including those containing solid molecular nitrogen (Sobolev et al., 2019a). In synthetic diamond monocrystals, inclusions with octahedral morphology were produced by the temperature differential method (Palyanov et al., 1994).

SAMPLES

Samples for measuring the orientation of inclusion were selected based on maximally full representation of the most important minerals included in diamonds of the most typical, peridotitic paragenesis of inclusions. The most common inclusion mineral is known to be high-magnesium olivine with the forsterite content Fo [100Mg/(Mg+Fe)] from 91 to 94 (Sobolev et al., 2008, 2009b). Olivine is present in half of sixteen selected samples in an amount of one to seven inclusions (Table 1). Compared to most previous studies (Nestola et al., 2011, 2014, 2019; Neuser et al., 2015; Bruno et al., 2016; Milani et al., 2016; Nimis et al., 2016; Seryotkin et al., 2017; Hwang et al., 2018), certain samples contain, besides olivine, pyrope inclusions (samples 3636 and 3811 from diamonds of the Udachnaya pipe) and even a three-mineral association comprising, in addition to olivine and pyrope, also magnesiochromite (sample 3811 from the Udachnaya diamond pipe) (Table 1). Special attention in current studies is given to magnesiochromite (Chr) inclusions that are present (from one to thirteen inclusions) in seven studied samples, which accounts for almost half of the entire sample and confirms the widespread occurrence of spinelide inclusions in diamonds (Table 1).

Table 1. Diamond samples used for measurements of inclusions orientation

N	Locality kimberlite pipe	Sample	Mineral inclusions		
			Ol	Prp	Chr
1	Udachnaya	3273	1	–	4
2	Udachnaya	3636	5	3	–
3	Mir	Mir-616-1	–	1	–
4	Mir	Mir-616-2	–	1	–
5	Mir	MRL-38	1	–	–
6	Mir	MRL-39	7	–	–
7	Mir	MRL-40	1	–	–
8	Udachnaya	3811	1	5	1
9	Udachnaya	UDK-1	–	–	6
10	Udachnaya	UDK-2	–	–	13
11	Internatsionalnaya	INS-1	–	–	5
12	Internatsionalnaya	INS-24	–	–	6
13	Internatsionalnaya	INS-50	–	–	3
14	Aikhal	Aih-1	–	3	–
15	Yubileynaya	Ubc-1-1	3	–	–
16	Yubileynaya	Ubc-1-2	3	–	–
Total		76*	22	13	38

Note: Ol, olivine; Prp, Cr-pyrope; Chr, magnesiochromite after (Whitney and Evans, 2010); samples Mir-616-1 and Mir-616-2 represent fragments of the same crystal containing one pyrope inclusion each.

*Added data on orientation of three olivine inclusions from sample 3226, Fig. 4.

METHODS

The orientations of inclusions in each diamond were determined by single-crystal X-ray diffractometry using a Stoe STADI IPDS 2T single-crystal diffractometer (MoK_α radiation, 50 kV, 30 mA, graphite monochromator, 0.3 mm collimator). The sample–detector distance was 100 mm. Diamonds were glued onto a glass thread and mounted on a diffractometer head. In the case of tightly-packed inclusions, the optical alignment was performed using one of them. All grouped inclusions were within the X-ray beam, and their diffraction data were accumulated in one experiment. The estimated crystal orientation error due to crystal shift from the X-ray beam center did not exceed 2° (Nestola et al., 2014). If the inclusions were far from each other, and there was a risk that an inclusion would be outside of the beam, each inclusion was adjusted and measured individually. The diffraction array was accumulated in the full reflection sphere using omega-scanning with a scan width of 1°/frame. Sets of 2D diffraction frames were processed using the CrysAlisPro 171.38.43 software (Agilent).

The relative orientation of inclusions in diamonds was determined using the OrientXplot 4.2 software (Angel et al., 2015a,b). Comparison of relative orientations of inclusions in different diamonds should consider an ambiguous choice

of crystallographic directions of the inclusion and the diamond due to their symmetry. This uncertainty is eliminated by recalculating the orientation matrices for each inclusion and the host diamond using appropriate symmetry operations; as a result, a chosen crystallographic direction of the inclusion occurs in the indicated crystallographic asymmetric diamond unit (Nestola et al., 2014). The obtained orientation of all inclusions in the diamond coordinate system is shown in Fig. 2; the recalculated angles between the coordinate directions of the inclusions and the host crystal are given in Table 2.

RESULTS

Crystallographic orientation of inclusions

The orientation of 76 mineral inclusions was measured in a total of 16 diamond crystals from the major primary deposits (kimberlite pipes) of Yakutia. Despite the fact that olivines are the most common inclusions whose orientation relative to diamond, increased attention in recent publications (Nestola et al., 2011, 2014; Neuser et al., 2015; Bruno et al., 2016; Milani et al., 2016; Nimis et al., 2016; Seryotkin et al., 2017; Hwang et al., 2018), the tested collection was selected to represent the most typical minerals in diamonds belonging to the predominant peridotitic paragenesis for most kimberlites. The main minerals of this paragenesis, along with the markedly predominant olivine, include pyrope and magnesiochromite (Nimis et al., 2019). Pyroxenes were present in subordinate numbers and were not available in the collection. In addition to single crystal X-ray diffractometry, diffraction of backscattered electrons was also used (Neuser et al., 2015).

Figure 2 presents the results of analysis of 76 inclusions by single-crystal X-ray diffractometry: olivine (25 inclusions), pyrope (13 inclusions), and magnesiochromite (38 inclusions) from 16 diamond samples in the sequence indicated in Table 1. The tested diamond samples contained various combinations of olivine, pyrope, and magnesiochromite (chromite) inclusions, single and multiple inclusions of one of the listed minerals. This set of inclusions was studied for the first time. According to single-crystal X-ray diffraction analysis, the angles between crystallographic directions of inclusions and diamond in the same sequence are presented in Table 2.

The novelty of the approach used to study the relative orientation of inclusions and diamond lies in the first applied special selection of diamond samples containing not only olivine but also typical minerals of the peridotitic diamond paragenesis, such as pyrope and magnesiochromite. Most (10) of the tested diamonds belong to the major deposits of Yakutia: Udachnaya and Mir kimberlite pipes of Paleozoic age (Kinny et al., 1997; Davis et al., 1980; Agashev et al., 2004; Schmitt et al., 2019) (Table 1).

Sample 3273 contains one olivine inclusion of the octahedral morphology related to the influence of the host diamond as well as four magnesiochromite inclusions. The second sample from the same Udachnaya pipe contains five olivine inclusions and three pyrope inclusions. Of the four magnesiochromite inclusions in sample 3273, two have axis orientations parallel to the axes of the host diamond. Five olivine inclusions in sample 3636 are oriented randomly, without any regularities.

Two fragments of the Mir-616 diamond (Mir 616-1 and Mir 616-2) contain one purple pyrope inclusion each, which are oriented without any regularities (Fig. 2). The angles between coordinate directions of the inclusion and the matrix of inclusions are about 30°. In the first sample, the angle between [111] diamond and [111] garnet is 7.7°, which does not obviously indicate anything for random orientations of the coordinate axes. In the second, this angle is 36.6°. The angles between coordinate axes of the inclusion and the host diamond for samples Mir 616-1 and Mir 616-2 are presented in Table 2.

Two diamonds (MRL-38 and MRL-40) contain one olivine inclusion each, and the MRL-39 sample contains seven olivine crystals. Table 2 presents the angles between coordinate axes of the host diamond and the inclusions. The olivine orientation relative to the diamond axes is shown in Fig. 2. The stereograms show the orientation of inclusions relative to the crystallographic directions of the diamond, which is re-calculated with allowance for the symmetry of the inclusion crystals and the matrix.

Obviously, epitaxial growth of the inclusion mineral and the host mineral suggests their certain orientation relative to each other. In the case of olivine, it is argued that the (010) olivine and (111) diamond planes as well as the [101] olivine and [101] diamond directions should coincide (Hartman, 1954) due to a possible epitaxial matching based on the similar period lengths in these directions in olivine and diamond structures on their contact planes.

In the MRL-38 and MRL-40 samples, the orientation of olivine crystals relative to the host diamond may be called random (Fig. 2). For example, in MRL-38, the angle between the olivine b axis and the [111] diamond direction is 17°, and the angle between [101] olivine and [101] diamond is 12.5°. In MRL-40, the angles are even greater. Olivine inclusion No. 6 in MRL-39 displays coincidence of the b axis with the [111] direction of diamond: the angle between them is 0.3°. However, the second olivine direction, [101], forms an angle of 29.0° with the closest [101] diamond direction (namely [–101]), which does not suggest their possible joint growth. The orientation of the other six olivine inclusions also does not suggest their syngenicity.

Sample 3811 is a large (up to 1 cm) crystal strongly flattened in the [111] direction; it contains 5 garnet crystals, one olivine crystal, and one spinelide crystal. Table 2 shows the angles between coordinate axes of the host diamond and the inclusions. The orientation of the crystallographic axes of inclusions relative to the diamond axes is shown in Fig. 2.

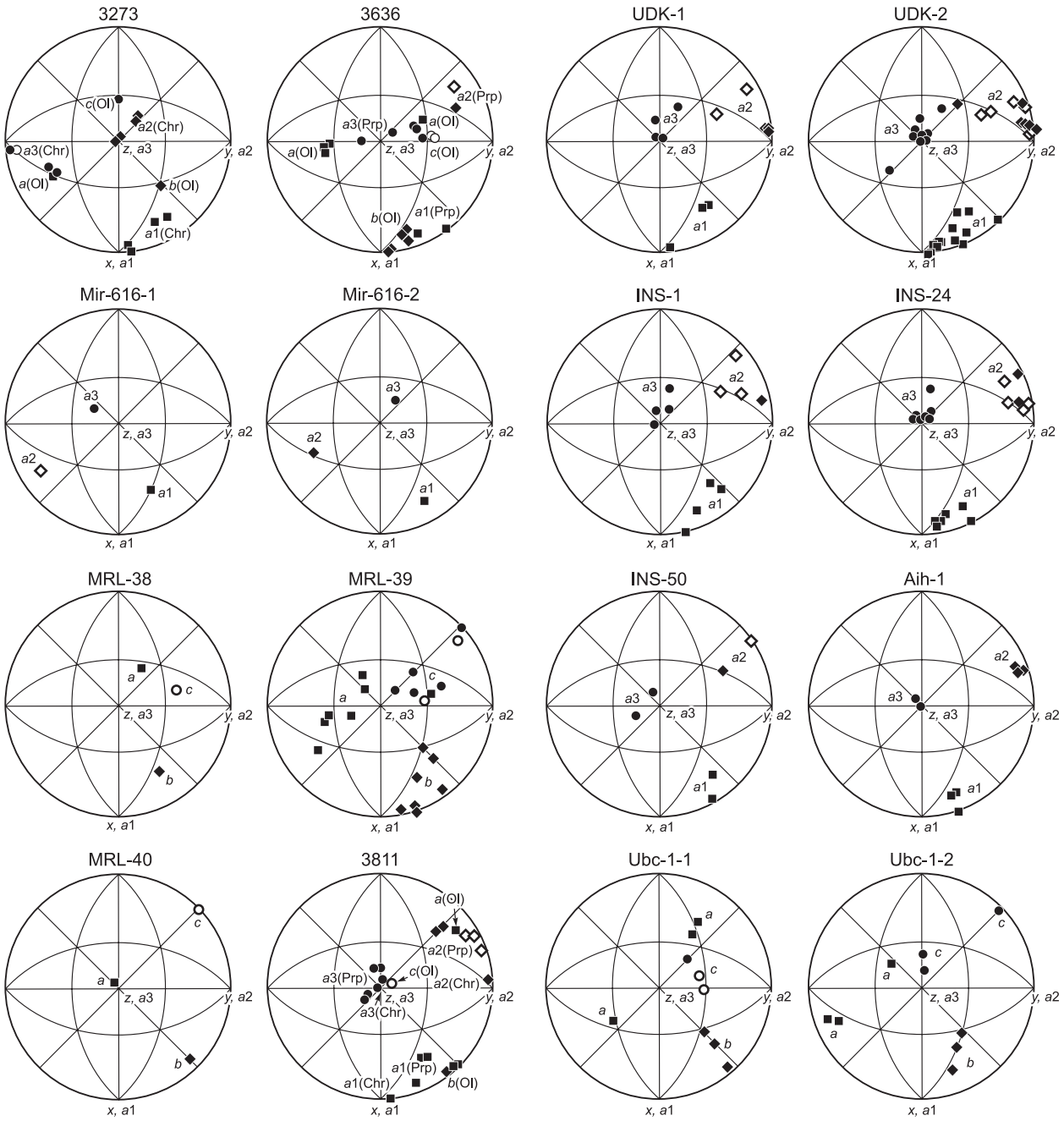

Fig. 2. Orientation of olivine (Ol), pyrope (Prp), and magnesiochromite (Chr) inclusions in the crystallographic system of a host diamond in studied samples. The diamond axes are directed as follows: a1 – downward, a2 – to the right, a3 – according to the rule of the right coordinate system. The axes a (a1), b (a2), and c (a3) of inclusions are denoted by squares, rhombuses, and circles, respectively. The filled and hollow symbols mark the positive and negative direction of the vector, respectively. The sequence of samples is identical to the order shown in Table 1.

Neither the garnet inclusions nor the olivine crystal, given their location in the host diamond, displays any regular orientation. However, the crystallographic axes of magnesiochromite are oriented almost parallel to the diamond axes: the angles between them do not exceed 6°. It should be noted that the estimated error in determining the crystal orientation when it is shifted from the center of the X-ray beam does not exceed 2° (Nestola et al., 2014). However, it should be noted that the error in determining the orientation of diamond increases as its size grows because the diamond necessarily occurs beyond the X-ray beam. In this case, the diamond, unlike the tested inclusion, is not centered, which also reduces the accuracy of determining it and the orientation matrix. Given these facts, it may be concluded that the differences in the direction of spinelide and diamond axes are at least close to the determination error.

Table 2. Angles between the three axes of minerals and three axes of diamonds for inclusions studied in this work

Diamonds axes	*a*1			*a*2			*a*3		
Inclusion axes	*a*1 (*a*)	*a*2 (*b*)	*a*3 (*c*)	*a*1 (*a*)	*a*2 (*b*)	*a*3 (*c*)	*a*1 (*a*)	*a*2 (*b*)	*a*3 (*c*)
3273									
Olivine	64.81	52.96	132.48	144.53	54.54	89.75	66.77	56.76	42.48
Chromite 1	6.44	94.48	85.38	85.29	89.13	175.21	85.61	4.56	88.76
Chromite 2	27.98	110.94	72.31	65.87	74.42	150.72	76.70	26.56	67.46
Chromite 3	34.08	113.72	67.04	58.53	72.47	142.93	78.26	30.17	62.65
Chromite 4	5.28	91.19	84.86	84.96	94.13	173.47	88.45	4.30	94.01
3636									
Olivine 1	80. 46	15.68	102.33	142.83	75.03	56.89	54.48	85.44	35.91
Olivine 2	87.50	3.58	92.55	139.85	86.44	50.07	49.96	89.65	40.05
Olivine 3	108.85	19.28	93.90	51.00	74.45	43.16	45.02	78.88	132.89
Olivine 4	84.60	15.11	104.07	145.02	77.66	57.86	55.56	81.42	35.80
Olivine 5	94.49	5.58	93.32	48.90	84.54	41.62	41.45	88.83	131.43
Pyrope 1	22.65	112.64	89.83	68.77	30.07	110.25	82.49	71.30	20.26
Pyrope 2	36.44	125.29	97.95	53.56	38.43	79.45	89.85	103.27	13.27
Mir-616-1									
Pyrope	34.73	103.80	58.84	65.84	112.61	145.83	66.66	26.90	102.62
Mir-616-2									
Pyrope	32.14	112.37	68.17	60.73	73.68	145.67	77.89	28.23	64.92
MRL-38									
Olivine	125.59	38.61	103.03	69.28	60.47	37.35	42.92	67.49	124.28
MRL-39									
Olivine 1	81.78	32.17	120.86	140.23	65.07	61.23	51.42	71.01	44.70
Olivine 2	80.74	18.54	105.92	119.88	71.47	36.23	31.57	89.61	58.43
Olivine 3	58.13	36.27	105.47	140.76	54.13	76.23	69.62	85.36	20.95
Olivine 4	106.45	49.42	134.81	106.26	49.71	44.81	23.46	66.54	90.06
Olivine 5	77.05	18.29	102.69	142.68	72.04	58.53	55.71	86.69	34.50
Olivine 6	119.54	54.52	130.39	108.20	54.75	41.01	35.71	54.94	95.93
Olivine 7	100.17	11.25	94.75	43.55	79.25	48.45	48.24	86.73	138.05
MRL-40									
Olivine	95.74	45.38	134.80	94.42	45.52	44.82	7.26	82.80	90.91
3811									
Pyrope 1	43.33	132.32	82.36	46.87	46.05	103.06	86.57	75.21	15.20
Pyrope 2	21.31	109.95	97.19	69.73	20.31	88.76	83.68	93.64	7.30
Pyrope 3	44.97	132.22	77.37	45.13	49.21	105.95	87.60	69.59	20.56
Pyrope 4	35.06	118.58	108.55	61.77	28.91	95.70	70.98	93.97	19.47
Pyrope 5	37.11	121.00	108.33	57.88	32.21	92.14	73.43	97.90	18.46
Chromite	**5.04**	**94.70**	**91.83**	**85.42**	5.76	93.49	87.89	86.67	3.94
Olivine	127.79	37.98	93.20	39.41	52.23	80.38	80.45	86.60	169.85
UDK-1									
Chromite 1	6.21	84.56	87.01	95.57	6.11	87.51	92.74	92.77	3.90
Chromite 2	37.56	59.27	70.58	120.20	31.09	96.71	110.14	94.28	20.63
Chromite 3	39.85	56.36	71.22	110.02	38.79	121.64	122.79	72.99	37.99
Chromite 4	7.07	83.77	86.68	96.09	6.62	92.60	93.58	87.77	4.22
Chromite 5	6.00	84.51	87.60	95.36	6.13	92.96	92.67	87.28	3.82
Chromite 6	6.42	84.21	87.23	95.63	6.46	93.15	93.07	87.14	4.20

(*continued on next page*)

Table 2. (*continued*)

Diamonds axes	*a*1			*a*2			*a*3		
Inclusion axes	*a*1 (*a*)	*a*2 (*b*)	*a*3 (*c*)	*a*1 (*a*)	*a*2 (*b*)	*a*3 (*c*)	*a*1 (*a*)	*a*2 (*b*)	*a*3 (*c*)
UDK-2									
Chromite 1	11.45	80.61	83.51	100.11	11.97	83.67	95.32	97.35	9.09
Chromite 2	3.47	86.56	89.53	93.41	4.62	93.11	90.65	86.93	3.14
Chromite 3	8.49	82.34	86.37	97.88	8.58	86.64	93.14	93.82	4.95
Chromite 4	18.93	71.82	84.90	107.90	18.27	93.55	95.95	88.21	6.21
Chromite 5	11.90	79.85	83.86	99.44	11.53	96.55	97.18	84.60	9.00
Chromite 6	5.60	85.02	87.45	94.95	5.00	90.70	92.60	89.52	2.64
Chromite 7	43.92	46.14	88.07	122.16	58.61	48.14	63.59	119.91	41.93
Chromite 8	26.43	64.51	83.47	110.89	32.15	113.26	105.44	71.76	24.27
Chromite 9	8.13	84.01	84.52	96.01	6.01	90.01	95.45	90.56	5.48
Chromite 10	37.13	58.13	72.99	109.38	37.97	121.21	120.27	71.58	36.51
Chromite 11	19.03	71.72	84.89	108.01	18.36	93.44	95.93	88.32	6.17
Chromite 12	32.45	65.95	69.58	112.59	24.08	97.89	112.00	91.04	22.02
Chromite 13	22.55	71.35	77.78	109.79	20.09	86.65	100.37	97.22	12.68
INS-1									
Chromite 1	13.72	76.28	89.68	103.69	14.62	84.99	89.13	94.94	5.02
Chromite 2	45.39	47.72	76.54	131.99	42.65	96.16	104.08	94.61	14.85
Chromite 3	25.36	67.24	79.40	109.47	25.22	105.39	105.61	79.72	18.84
Chromite 4	45.40	52.92	67.75	115.18	38.57	117.12	124.81	80.85	36.34
INS-24									
Chromite 1	12.82	78.83	83.80	101.86	13.52	83.61	94.79	97.51	8.92
Chromite 2	27.10	62.94	88.70	116.42	28.46	99.83	95.60	81.85	9.91
Chromite 3	17.75	75.09	80.59	102.62	18.17	102.86	102.28	79.85	16.03
Chromite 4	10.38	80.58	85.69	99.37	9.43	91.02	94.42	89.69	4.43
Chromite 5	10.29	82.19	83.34	97.30	8.66	94.63	97.22	86.29	8.12
Chromite 6	28.85	63.28	79.93	117.39	27.42	88.76	98.36	95.70	10.14
INS-50									
Chromite 1	39.28	55.38	73.77	126.05	36.06	90.78	103.51	98.85	16.25
Chromite 2	39.32	55.33	73.79	126.09	36.10	90.80	103.51	98.84	16.23
Chromite 3	28.75	61.69	85.39	117.10	40.06	62.96	81.14	115.80	27.49
Aih-1									
Pyrope 1	21.25	71.46	79.99	109.55	20.07	85.64	97.99	97.41	10.94
Pyrope 2	19.24	70.77	89.66	109.24	19.28	88.72	89.90	91.32	1.33
Pyrope 3	24.65	67.99	79.46	113.22	23.76	85.22	97.83	98.50	11.60
Ubc-1-1									
Olivine 1	62.89	130.05	52.04	40.14	50.44	84.27	117.12	64.86	38.54
Olivine 2	143.64	62.82	67.79	53.68	53.71	56.85	88.51	48.38	138.34
Olivine 3	136.72	64.14	58.07	48.92	48.39	69.10	101.28	52.61	140.36
Ubc-1-2									
Olivine 1	70.89	158.31	80.13	25.58	68.81	76.34	106.35	85.56	16.97
Olivine 2	111.04	115.76	34.31	52.63	55.69	55.92	135.16	45.38	86.48
Olivin 3	68.40	152.50	73.81	40.26	62.64	62.97	122.09	87.40	32.22
3226*									
Olivine 1	70.68	42.01	54.42	56.16	36.96	76.91	106.71	49.99	135.23
Olivine 2	90.62	51.72	141.72	122.33	56.38	129.66	114.35	54.13	45.76
Olivine 3	160.67	75.33	77.70	129.45	76.45	42.63	30.17	60.45	84.46

Note: *Additionally the orientation of three largest olivine inclusions are determined in this sample (Fig. 4*D*). In the samples 3811, UDK-1 and UDK-2 chromite (magnesiochromite) inclusions with orientation close to regular are highlighted.

Six magnesiochromite crystals are present in the UDC-1 sample, four of which have an orientation close to that of the host diamond. The angles between crystallographic axes of the diamond and the magnesiochromite are within a range of 3.8–7.1°, which suggests their regular orientation. The angles between the [111] directions of the diamond and the magnesiochromite for four regularly oriented inclusions amount to 5.8–7.4°. The other two inclusions are oriented randomly; the angles between coordinate directions of the magnesiochromite and he diamond are greater than 20°.

In the UDC-2 sample, 13 spinelide crystals of very different orientations are found (Fig. 2). The angles between the appropriate coordinate directions of the inclusion and the diamond vary in a range of 3–60° (Table 2). Correspondingly, the angle between the [111] directions of inclusions and the host diamond is 4.6–43.7°. Inclusions Nos. 2 and 6 have a presumably regular orientation; the others are randomly oriented.

The INS-1 sample contains 5 randomly oriented spinelide (magnesiochromite) inclusions (Fig. 2). The angles between the coordinate axes of the inclusion and the diamond range from 5 to 45°.

Six spinelide inclusions are found in the INS-24 sample. Their orientation cannot be classified as regular (Table 2). For example, even if one of the angles between the appropriate coordinate axes is small, the angles between the other axes are close to or more than 10°, which excludes any regularity in the location of this inclusion in the host diamond. The angles between the [111] directions of the matrix and inclusions vary in a range of 10.0–27.5°.

The INS-50 sample contains three spinelide inclusions, two of which are oriented almost identically; the difference in angles is less than 1°. It may be supposed that this is a single split crystal. The orientation of crystals relative to the diamond is random.

Three pyropes randomly oriented relative to the host diamond are found in the Aih-1 sample. The Ubc-1 sample contains three olivines. The diamond is a spinel twin. Table 2 and Fig. 2 show the orientation of inclusions for each block. A similar crystal is shown in Fig. 4.

In the present experiment involving sixteen diamond crystals (Table 1), there is no inclusion whose orientation meets the epitaxial criterion (Hartman, 1954).

GEOCHEMICAL FEATURES OF INCLUSIONS AND HOST DIAMONDS

The role of carbon isotope composition of diamonds in characterization of diamond-forming medium

One of the main characteristics of natural diamonds is the carbon isotope composition. After the discovery of diamonds in the Siberian Platform, active research has been organized at the Institute of Geochemistry and Analytical Chemistry (Galimov, 1984); diamonds from other deposits, mainly from South Africa, have been studied in the USA (Deines, 1980). Intensive investigation of mineral inclusions in diamonds (see the Introduction) has proved a clear dependence of variations in the carbon isotopic composition of diamonds on the paragenesis of their mineral inclusions, the main of which are peridotitic and eclogitic. This evidence was first obtained based on analysis of the carbon isotope composition in 86 diamond samples with well-defined paragenesis of inclusions (Sobolev et al., 1979). The carbon isotope composition of peridotitic diamonds was in the $\delta^{13}C$ range from –2 to –8‰ PDB, and that of eclogitic diamonds, including diamonds with kyanite and coesite, was from + 2 to –25‰ PDB. The observed pattern was fully preserved upon further accumulation of material up to 1000 analyzes (Cartigny, 2005) and 2500 analyzes (Shirey et al., 2013; Cartigny et al., 2014) of diamonds containing mineral inclusions. This clear pattern indicates a significant correlation between the isotopic composition of diamonds and the paragenesis of diamond inclusions and, therefore, the syngenetic nature of the inclusions.

Xenoliths of diamondiferous peridotites and eclogites

The rarest samples from the deepest-seated rocks include diamondiferous pyrope peridotites. Information and generalizations of data on these rocks, which have been made in different years (Sobolev et al., 1969b; Ilupin et al., 1982; Sobolev et al., 1984; Barashkov and Zudin, 1997; Creighton et al., 2008; Logvinova et al., 2015; Sobolev et al., 2019b), indicate the rarity of these xenoliths compared to diamondiferous eclogite xenoliths because olivine that constitutes the bulk of the rock is usually serpentinized, which leads to rock disintegration. However, these rocks, similar to diamondiferous eclogites, are important for comprehensive consideration of the problem of protogenetic and syngenetic inclusions in diamonds. It is necessary to carefully approach identification of similar pyrope and diamond relationships in diamondiferous peridotites taking into account possible identification of diamond inclusions in olivine and pyrope, especially in samples from an unaltered kimberlite of the Udachnaya-Vostochnaya pipe. It is extremely important to consider relationships for the mineral association of the unique megacrystalline peridotite xenolith from the Udachnaya pipe (Ilupin et al., 1982), which is a 2 cm olivine megacrystal comprising two octahedral diamond crystals, one of which contains olivine with Fo 93.6, while the host olivine is characterized by Fo 93.2, as well as a magnesiochromite inclusion. The host olivine comprises a subcalcium pyrope inclusion whose composition is similar to that of inclusions in diamonds (Cr_2O_3 – 11.6 wt.%; CaO – 3.54 wt.%). Given the differences in the Fo content in the host olivine and the diamond-hosted olivine, it may be concluded about a higher temperature nature of the inclusion and a syngenetic ratio of the diamond and the olivine inclusion. A similar conclusion on the syngenetic nature of pyrope with re-

spect to the pyrope-hosted diamond may be made for a microxenolite sample of diamondiferous peridotite from the Diavik pipe, Canada (Creighton et al., 2008), where the diamond is completely enclosed in the pyrope. An example of Al_2O_3 paste-polished diamond completely enclosed in pyrope was described in polycrystalline diamond aggregates (PDAs) from South Africa, diamondites (Mikhail et al., 2019), which proves the syngenetic nature of pyrope.

In diamonds and associated garnets and olivines, of great significance are fluid inclusions in which saturated hydrocarbons dominate (Sobolev, 1960; Sobolev et al., 2018; 2019a,b). The H_2O impurity in these minerals is extremely low, which is confirmed by SIMS analyses for olivines included in diamonds (Jean et al., 2016). Hydrocarbons obtained experimentally at high pressures (McCollom, 2013; Sephton and Hazen, 2013; Etiope and Schoell, 2014; Sokol et al., 2020; Truche et al., 2020) were found in natural samples of diamonds and associated minerals (Sobolev et al., 2019b). The earliest diagnostics of light hydrocarbons, presumably C_2H_2, was made in diamond using the IR spectrum (band 3107 cm^{-1}) (Sobolev and Lenskaya, 1965; Sobolev, 1989). However, the capabilities of IR (infrared) and Raman spectroscopy are not always considered when studying deep-seated xenoliths. For example, in a paper devoted to detailed characterization of megacrystalline xenoliths of dunites in kimberlite (Pernet-Fisher et al., 2019), the authors indicate abundance of fluid and melt inclusions in olivine, but do not try to characterize them. This reduces the significance of appropriate studies of xenoliths, in particular because megacrystalline dunites and harzburgites can belong to different depth facies: graphite and diamond (Sobolev, 1977; Rodionov and Sobolev, 1985; Pearson et al., 1994; Sobolev et al., 2019b).

Significant amounts of diamondiferous eclogite xenoliths are known to occur in kimberlites. In many eclogite samples, especially in large ones, there are complex relationships between primary minerals and diamonds, often containing garnet and pyroxene inclusions, indicating multi-stage diamond formation (Sobolev et al., 1972; Ireland et al., 1994; Taylor et al., 1996, 2000; Sobolev et al., 1998b; Misra et al., 2004; Stepanov et al., 2007; Liu et al., 2009; Howarth et al., 2015; Shatsky et al., 2016). In some eclogite samples, in particular from the Udachnaya pipe (Howarth et al., 2015), 3D tomography in pseudo thin sections clearly identifies diamond completely enclosed in garnet, while other diamonds occur in the intergranular space. This relationship of garnet and diamond completely enclosed in the garnet indicates an early diamond-forming event and, therefore, the syngenetic nature of the garnet.

DISCUSSION

Among natural minerals, it is difficult to select examples of diamond-like solid inclusions whose shape is completely induced by the host crystal. Usually, natural crystals contain crystalline mineral inclusions whose morphology reflects the formation of a compromised shape in the form of an induction surface of joint growth. A similar form of growth is also typical of individuals in contact with each other, which are developed in druses, disoriented crystal intergrowths, and graphic intergrowths of minerals (Grigor'ev, 1961; Lemmlein, 1973). The very fact of the existence of a diamond-imposed shape of syngenetic inclusions in a wide variety of minerals, regardless of their own chemical composition, intrinsic crystal structure, symmetry, and crystallographic faceting, emphasizes the uniqueness of conditions for their co-crystallization with diamond. One of the favorable causes is the lack of isomorphic miscibility of the chemical elements comprising inclusions and diamond. For other minerals, similar conditions for the formation of syngenetic inclusions are rare. In addition, an extremely high density of the diamond crystalline packing and associated high crystallization pressure create favorable conditions for transfer of the diamond morphology to inclusions in contact with the diamond. This is partially confirmed by numerous examples of a regular geometric shape of gas-liquid inclusions in minerals giving low resistance to the host crystal during growth. For example, in crystals of many minerals (garnet, quartz, topaz, beryl), the cavities hosting them acquire an internal faceting that fully corresponds to the crystallographic forms and symmetries of the host mineral. Probably, step ends and growth layers of the diamond also did not encounter significant resistance from mineral inclusions during crystallization, and the diamond was able to freely transfer its faceting elements to the surface in contact with it.

In recent years, an active discussion about relationships between diamond and its mineral inclusions has rarely addressed the issue of a complex diamond growth pattern revealed by the cathodoluminescence (CL) method. Multistage growth alternating with dissolution is also characteristic of kimberlite minerals such as olivine whose zone number fixed by variable contents of impurity elements can reach or even exceed ten (Sobolev et al., 2008, 2009). Several publications (Bulanova, 1995; Sobolev et al., 1998; Bulanova et al., 2002, 2014; Logvinova et al., 2005; Wiggers de Vries et al., 2011, 2013) have convincingly demonstrated that mineral inclusions, in particular magnesiochromites and garnets, including Cr-pyrope and Mg-Fe garnets, occurring in different growth zones of diamond can have different compositions. Composition differences were found not only for major but also for trace elements (Shimizu and Sobolev, 1995; Stachel et al., 2004; Logvinova et al., 2005; Stachel and Harris, 2008). Despite multidirectional changes in the composition of magnesiochromites from different diamond zones (Fig. 3), a tendency to increase Cr# and decrease Mg# is preserved in most cases. Chromium spinelides included in diamonds are, on average, more magnesian than spinelides found on the surface of polycrystalline diamond aggregates

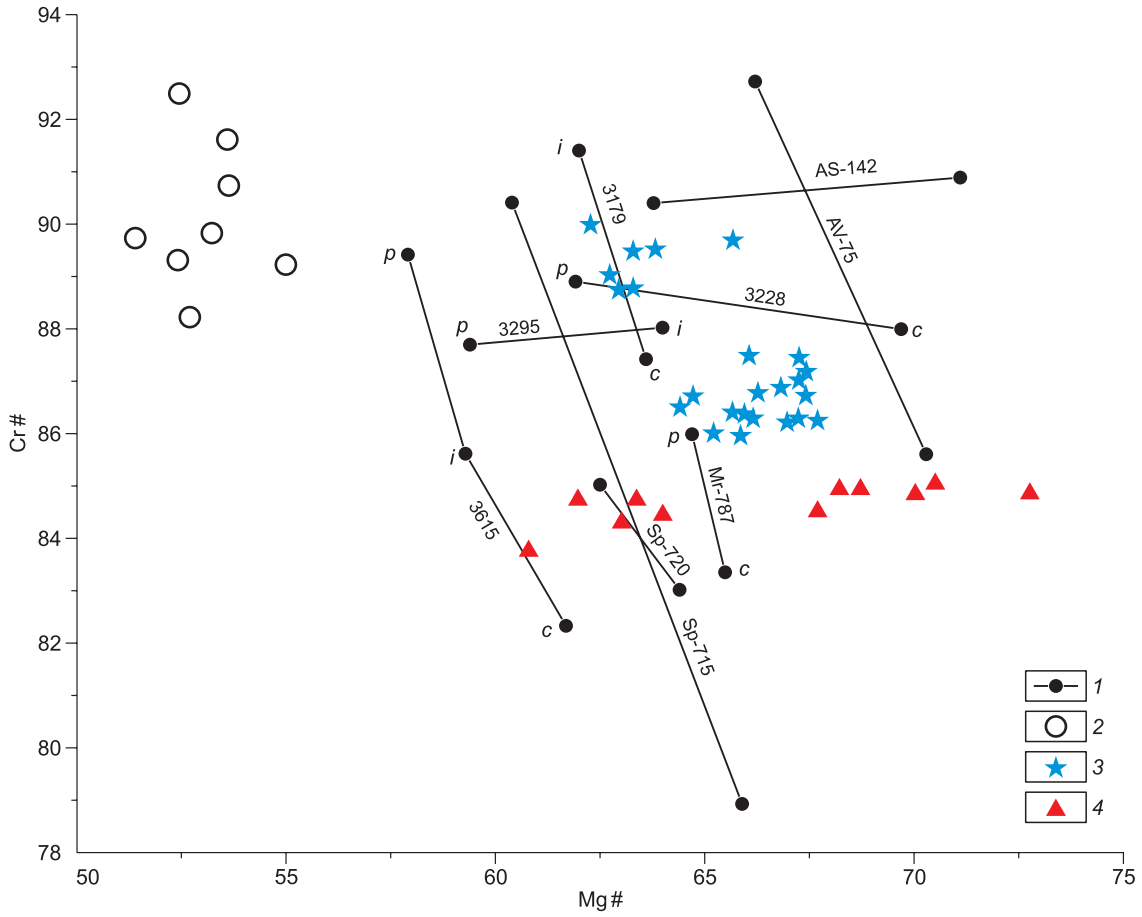

Fig. 3. Ratio of magnesium (Mg#) and chromium (Cr#) contents in spinelides included in Yakutian diamonds. Magnesiochromites from the central (c), intermediate (i), and peripheral (p) zones of diamond. Individual compositions from diamond zones (*1*); compositions of diamondiferous peridotites (*2*) from (Sobolev et al., 1984); from diamond UD-34 (*3*); from diamond Mr-761 (*4*). Mg# [100Mg(Mg+Fe^{2+})]; Cr# [100Cr(Cr+Al)]. Four-digit numbers of samples from diamonds from the Mir pipe (Bulanova, 1995). Samples from diamond from pipes Sputnik (Sp); Mir (AV and (Mr); Aikhal (AS). Data source: Bulanova (1995); Sobolev et al. (1997); Sobolev et al. (1984); Sobolev et al. (new data).

such as boart and framesite. This tendency is associated with a decrease in the crystallization temperature from inclusions in diamonds to magnesiochromites from polycrystalline diamond aggregates (Sobolev et al., 1989; Griffin et al., 1993; Bulanova, 1995) characterized by a lower mean $\delta^{13}C$ value of –4.5% PDB typical of the peridotitic paragenesis (Reutsky et al., 1999) and from diamondiferous peridotites (Sobolev et al., 1984; Sobolev et al., 1989). A wide Mg# range in the series of studied spinelides from Yakutian diamonds (Fig. 3) confirms an estimate of the temperature difference exceeding 400 °C towards a decrease upon growth of individual diamond crystals according to the distribution of Mg/Fe (O'Neill and Wall, 1987) and Zn impurity in spinelides (Griffin et al., 1993) within the range approximately from 1300 to 850 °C. Although individual diamond samples with abundant inclusions of eclogite garnets and pyroxenes, the total amount of which reached 40 (Sobolev et al., 1998a) and more than 20 with magnesiochromite inclusions (new data), have not been studied by CL (Fig. 3), a wide range of inclusion compositions indicates long-term joint growth and syngenetic nature of at least some of the inclusions. A convincing example is provided by both eleven magnesiochromite inclusions (Fig. 3, triangles) recovered by burning sample Mr-761, whose compositions differ only in variable Mg# values from 61 to 72.5, and their data points are located almost horizontally (Fig. 3), and 24 inclusions from sample UD-34 also recovered by burning the sample. Compositions of these inclusions indicated by asterisks, in contrast to most inclusions presented in Fig. 3, are located irregularly and grouped in two parts of the figure within two areas clearly separated from each other. Most of the spinelide composition data points (seventeen) are located in the area of Fig. 3 with reduced Cr# 86–88. This is probably due to a particularly complex growth pattern of diamond UD-34. Extraction of these amounts of inclusions of 10 to 200 μm in size can be performed only by burning the diamond and is of independent interest despite the impossibility to associate inclusions with individual zones of diamond growth.

Thirty-five composition data points of completely extracted individual magnesiochromite inclusions from two

diamond samples Mr-761 and UD-34 after their burning are indicated in Fig. 3 by colored symbols. They occupy about 30% of the total composition area of spinelides included in diamonds.

In an article by Agrosi et al. (2016), by using X-ray topography, a high-quality photograph of the olivine inclusion surface microrelief clearly demonstrates the growth step surface imposed by the diamond. A high-quality image shows all details of the inclusion surface and a regular step geometry corresponding to the octahedral faces.

A study (Nimis et al., 2016) suggested that a different morphology of inclusions may indicate their syngenetic nature (sharp-edged inclusions with clear induction surfaces), and rounded inclusions with dissolution traces may be protogenetic. Indeed, the large authors' collection of images contains clearly distinct sharp-edged octahedral inclusions of coesite, olivine, phlogopite (Sobolev et al., 2009a), and pyroxenes (Sobolev et al., 1999). Of particular note is the presence of an octahedral sharp-edged pyrope (Fig. 1) and an octahedral intergrowth of pyrope and chrome diopside (Sobolev et al., 1970) as well as octahedral monocrystals and polymineralic intergrowths of pyrope, olivine, and pyroxene (Sobolev et al., 1972). The last two mentioned studies reported not only monomineralic and polymineralic inclusions of garnets and pyroxenes with an octahedral morphology but also olivine inclusions having their own morphology (Fig. 1).

It should be emphasized that pronounced morphological traits of the syngeneticity of inclusions represented by a constrained crystallographic shape imposed by the host diamond (Schmitt et al., 2019; Sobolev and Yefimova, 2000) are found exclusively in crystals of an octahedral habit. For example, it is worth noting separately that a full cubic, apart from octahedral, faceting of mineral inclusions has not been observed in diamond cuboids. First of all, this is associated with the difference in the growth mechanism of octahedral and cubic crystals. It is known that diamond octahedra are characterized by a lamellar (tangential) growth mechanism, while diamond cuboids are characterized by a normal (fibrous) growth mechanism. Therefore, the ability to acquire a crystallographic shape is the feature of inclusions in type I diamonds with an octahedral zonal-lamellar crystal structure. Indeed, the dominant lamellar growth mechanism of these crystals affects their external morphology usually in the form of triangular stepped layers generated by one or more centers of growth of octahedral faces.

According to the P. Curie's principle, there is the dependence of symmetry distortion of the external shape of garnet and olivine inclusions on the position in the bulk of an octahedral host diamond relative to its sectorial-zonal structure. The inclusion shape is also found not to have a direct relationship with the mutual structural orientation of inclusions relative to crystallographic directions of the diamond (Ugap'eva et al., 2015). It is worth noting that many of the listed minerals, which display the diamond faceting of inclusions, also lack signs of epitaxial intergrowth with diamond, which once again confirms these exceptions (Figs. 4, 5).

Morphological features of inclusions in individual diamond crystals

Among sixteen studied crystals (Table 1; Fig. 4*C*), of particular interest is the morphology of inclusions found in spinel twins of diamond octahedra from Udachnaya (sample 3226, Fig. 4) and Mir (sample 616, Fig. 5) pipes. The effect of the twin boundary on the shape and orientation of inclusions has not been addressed in detail in studies of mineral inclusions in diamonds.

In the spinel twin from the Udachnaya pipe (sample 3226), diamond-hosted inclusions are represented by olivine, and all they are concentrated in only one of its crystalline components. Diamond crystals constituting the twin have the shape of laminar octahedra with a smooth face surface (Fig. 4*A*). Olivine inclusions also have mirror-smooth faces, and the edges between them have a straight, slightly smoothed surface (Fig. 4*B, C*). The faces of inclusions are easily indexed by their shape and a position parallel to the (111) octahedral faces of a diamond crystal (Fig. 4*D*). Also, the surface of inclusions contains less developed (100) hexahedral faces. The shape of inclusions has symmetrical distortions. In this case, the octahedral faces facing an external faceting of the host diamond are more significantly developed. Inclusions located closer to the top of the host octahedron are elongated towards the top. On the whole, the distorted shape of inclusions corresponds to coincidences with 3m symmetry elements of a growth pyramid of the diamond octahedron.

In the spinel twin (sample 616), garnet and olivine inclusions are also uniformly distributed in the plane parallel to the composition plane (Fig. 5*A*). In this case, the inclusions are located on either one or the other side of the twin boundary, reflecting the symmetry of two different components of the twin crystal. Apparently, their active nucleation and growth were affected by crystal structure deformation resulting from twinning. This idea is in accordance with the shape of inclusions, which clearly depends on their position relative to the twin boundary and the faceting elements of crystals constituting the twin (Fig. 5). The structure, geometry, and interaction of trigonal growth layers on the spinel twin surface indicate that the growth center is shifted relative to the geometric center towards one of its vertices. In Fig. 5*A*, it is directed towards the lower right vertex of the twin. A relatively large garnet inclusion (Fig. 5*A–E*) coincides with the growth center of the twin. Its volumetric shape has a 3m pyramidal external symmetry with the pyramid base in the form of an octahedron face facing the twinning plane. The shape of other inclusions is developed in accordance with their position in the twin components.

Remarkably, inclusions not only have the faceting geometrically similar to that of the host diamond but also dis-

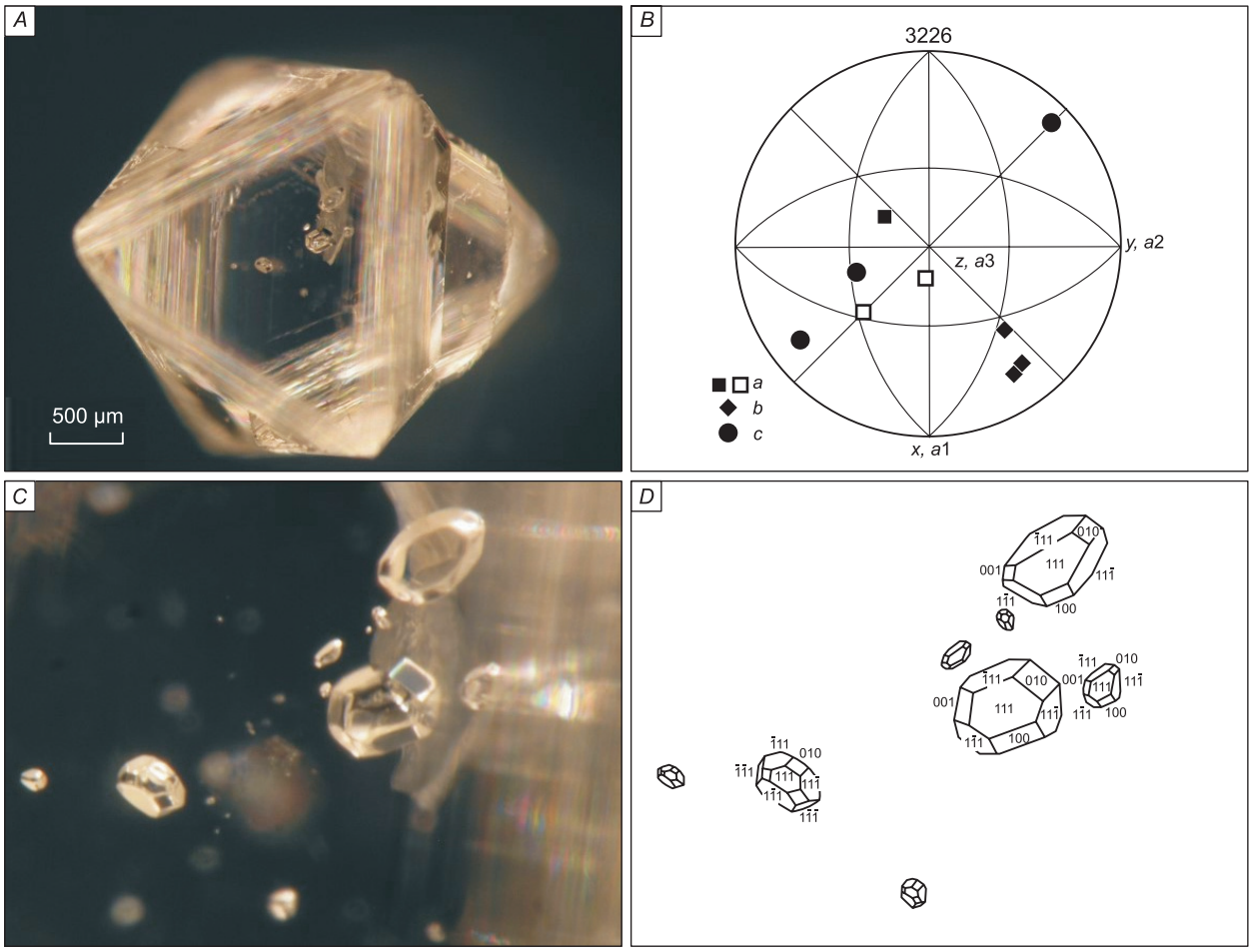

Fig. 4. Morphology of olivine inclusions in a spinel twin of diamond, which demonstrates a relationship with the position of inclusions relative to faceting elements of the host crystal. *A*, a general view of the twin; *B*, olivine inclusions photographed from the side of the octahedral face of the crystal; *C*, an enlarged fragment of the image in Fig. 4*B* with olivine inclusions; *D,* decoding of indices of the (111) octahedral and (100) hexahedral faces on the surface of olivine inclusions.

play a significant similarity of details of the surface microrelief. For example, the (111) octahedral faces in the central inclusion (Fig. 5*B, C, E*), as well as in the host diamond crystal, have a mirror-smooth surface. On the contrary, the (100) cube faces display a rough relief of the surface consisting of numerous octahedral vertices (Fig. 5*B–E*). The microrelief features present in this diamond sample are also observed in other garnet inclusions as well as in olivine inclusions. For example, a colorless isometric inclusion located at the octahedron apex has mirror-smooth (111) faces and roughly sculpted (100) faces (Fig. 5*B*). The second olivine inclusion is elongated along the edge of the host diamond crystal and has a shape consistent with the diamond surface and smooth (111) octahedral faces (Fig. 5*F*). The listed growth forms are typical of laminar octahedral crystals of natural diamond. The similarity of inclusion microrelief to the growth surface unambiguously indicates simultaneous growth of the diamond and the inclusion projecting the diamond shape.

CONCLUSION

A study of the crystallographic orientation of diamond and 76 olivine, magnesiochromite, and pyrope inclusions in 16 diamonds from the major primary deposits of Yakutia by single-crystal X-ray diffraction has not revealed any inclusion whose orientation meets the epitaxial criterion. Only individual magnesiochromite inclusions in three diamonds display an orientation close to the regular one.

The complex diamond growth history accompanied by its zoning, with wide variations in the composition of olivine, pyrope, Mg–Fe–Ca garnet, and especially magnesiochromite inclusions in different zones indicates a relationship between diamond growth and growth as well as variable composition of mineral inclusions of the main parageneses and possible coexistence of syngenetic and protogenetic mineral inclusions in the same diamond. Isolated diamond inclusions in olivine and pyrope of diamondiferous peridotite xenoliths and garnet of diamondiferous eclogites provide evidence of the syngenetic nature of these minerals with respect to diamond.

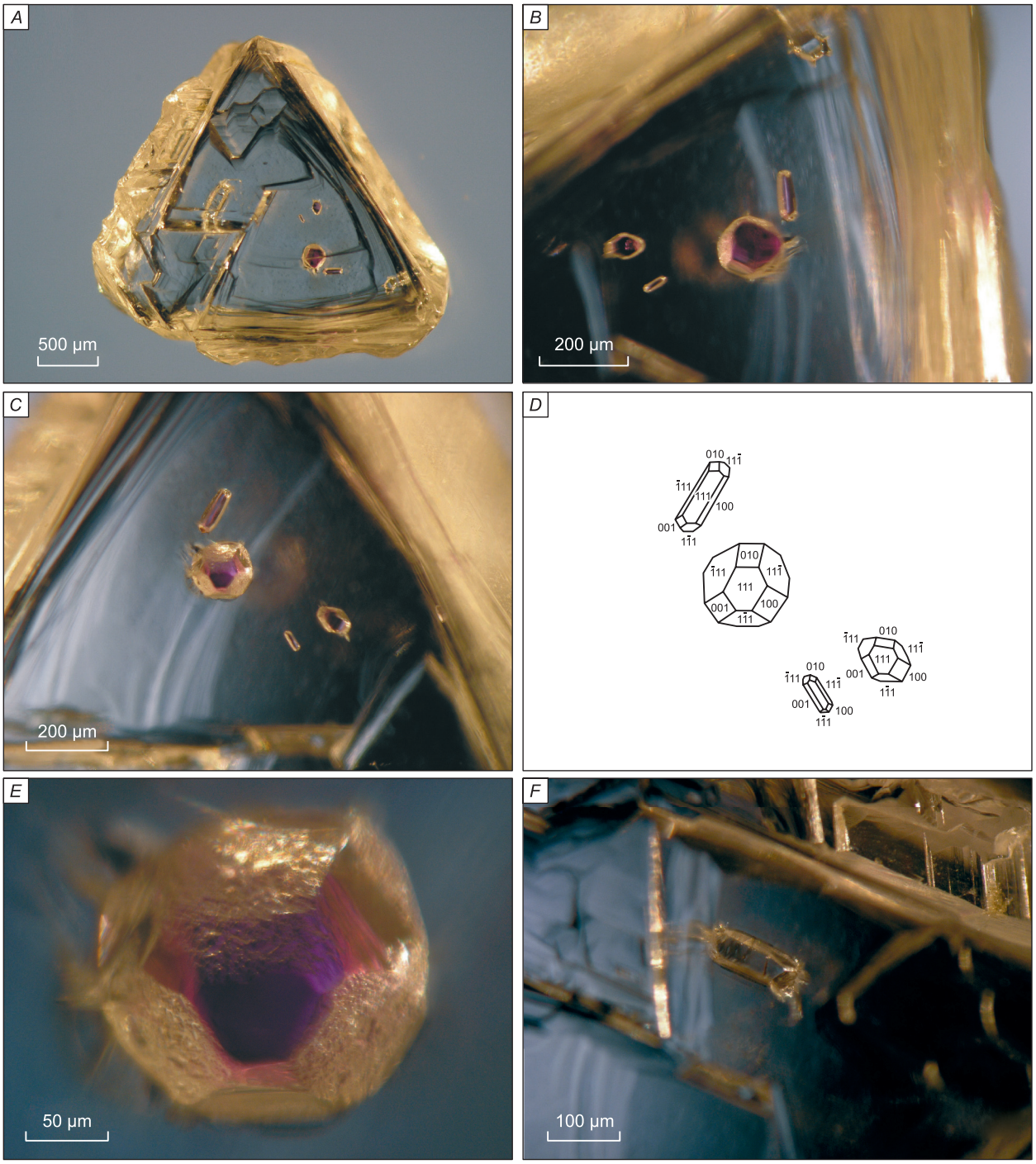

Fig. 5. Morphology of garnet and olivine inclusions in diamond, which demonstrates a relationship between their shape and the position of inclusions in the bulk of the host crystal (sample 616). A spinel twin of diamond with a displaced growth center: *A*, a general view of the twin; *B*, purple garnet inclusions and an olivine inclusion on the side facing the composition plane of diamond; *C*, the reverse side of garnet inclusions shown in Fig. *B*, which are exposed to the octahedral face of the diamond crystal; *D*, decoding of indices of the (111) octahedral and (100) hexahedral faces on the surface of garnet inclusions shown in Fig. *C*. The orientation of two elongated grains is measured (Table 2). *E*, a central garnet inclusion with mirror-smooth (111) octahedral faces and roughly sculpted (100) hexahedral faces; *F*, a colorless olivine inclusion elongated along the edge of a diamond octahedron.

A significant correlation between the carbon isotope composition and the type of diamond paragenesis (peridotitic and eclogitic) as well as the lack of a correlation with other diamond properties is one of the geochemical features.

Heavy hydrocarbons (rel.%), from pentane (C_5H_{12}) to hexadecane ($C_{16}H_{34}$), dominate in fluid inclusions in diamonds from kimberlites and placers as well as in pyrope and olivine of diamondiferous peridotite xenoliths.

The authors are sincerely grateful to reviewers S.V. Borisov and S.Z. Smirnov whose constructive comments have significantly improved the article.

This work is done on state assignment of IGM SB RAS and was supported by the Russian Science Foundation (RSF-19-17-00128) and the Russian Foundation for Basic Research (RFBR-17-05-00668).

REFERENCES

Agashev, A.M., Pokhilenko, N.P., Tolstov, A.V., Polyanichko, V.V., Malkovets, V.G., Sobolev, N.V., 2004. New age data on kimberlites from the Yakutian diamondiferous province. Dokl. Earth Sci. 399 (8), 1142–1145.

Agrosi, G., Nestola, F., Tempesta, G., Bruno, M., Scandale, E., Harris, J., 2016. X-ray topographic study of a diamond from Udachnaya: Implications for the genetic nature of inclusions. Lithos 248–251, 153–159.

Angel, R.J., Alvaro, M., Nestola, F., Mazzucchelli, M.J., 2015a. Diamond thermoelastic properties and implications for determining the pressure of formation of diamond–inclusion systems. Russian Geology and Geophysics (Geologiya i Geofizika) 56 (1–2), 211–220.

Angel, R., Milani, S., Alvaro, M., Nestola, F., 2015b. OrientXplot: a program to analyse and display relative crystal orientation. J. Appl. Crystallogr. 48, 1330–1334.

Arima, M., Harte, B., Sobolev, N.V., 2008. Preface: A special issue in honour of Vladimir S. Sobolev. Eur. J. Miner. 20 (3), 303–304.

Barashkov, Yu.P., Zudin, N.G., 1997. Composition of garnets with diamond inclusions from Krasnopresnenskaya kimberlite pipe, Yakutia. Geologiya i Geofizika (Russian Geology and Geophysics) 38 (2), 353– 357 (373–378).

Bartoshinskii, Z.V., Efimova, E.S, Zhikhareva, V.P., Sobolev, N.V., 1980. The crystall morphology of garnet inclusions in natural diamonds. Geologiya i Geofizika (Soviet Geology and Geophysics) 21 (3), 12–22 (9–17).

Bobrievich, A.P., Smirnov, G.I., Sobolev, V.S., 1959. Eclogite xenolith with diamonds. Dokl. Akad. Nauk SSSR, 126 (3), 637–640.

Bonney, T.G., 1899. The parent rock of the diamond in South Africa. Geol. Mag. 6, 309–321.

Borisov, S.V., Magarill, S.A., Pervukhina, N.V., 2020. Fedorov groups of crystallographic symmentry as algorithms of space and energy transformations in realization of stable atomic configurations. Crystallogr. Rep. 65 (1), 1–6.

Bruno, M., Rubbo, M., Aquilano, D., Massaro, F.R., Nestola, F., 2016. Diamond and its olivine inclusions: a strange relation revealed by ab initio simulations. Earth Planet. Sci. Lett., 435, 31–35.

Bulanova, G.P., 1995. The formation of diamond. J. Geochem. Explor. 53, 1–23.

Bulanova, G.P., Pearson, D.G., Hauri, E.H., Griffin, B.J., 2002. Carbon and nitrogen isotope systematics within a sector-growth diamond from the Mir kimberlite, Yakutia. Chem. Geol. 188 (1–2), 105–123.

Bulanova, G.P., Wiggers de Vries, D.F., Pearson, D.G., Beard, A., Mikhail S., Smelov, A.P., Davies, G.R., 2014. An eclogitic diamond from Mir pipe (Yakutia), recording two growth events from different isotopic sources. Chem. Geol. 381, 40–54.

Cartigny, P., 2005. Stable isotopes and the origin of diamond. Elements 1, 79–84.

Cartigny, P., Palot, M., Tomassot, E., Harris, J.W., 2014. Diamond formation a stable isotope perspective. Ann. Rev. Earth Planet. Sci. 42, 699–732.

Creighton, S., Stachel, T., McLean, H., Muehlenbach, S., Simonetti, A., Eichnberg, D., Luth, R., 2008. Diamondiferous peridotite microxenoliths from the Dravik diamond mine, NT. Contrib. Mineral. Petrol. 155, 541–554.

Davis, G.L., Sobolev, N.V., Kharkiv, A.D., 1980. New data on the age of Yakutian kimberlites (U-Pb zircon method). Dokl. Akad. Nauk SSSR, 254 (1), 175–179.

Dawson, J.B., 1984. Academician Vladimir Stepanovich Sobolev (1908–1982). Dedication. in: Kornprobst (Ed.), Kimberlites. Proc. of the Third Intern. Kimberl. Conf., Vol. 1: Developments in Petrology. Elsevier, Amsterdam.

Deines, P., 1980. The carbon isotopic composition of diamonds – relationship to diamond shape, color, occurrence and vapor composition. Geochim. Cosmochim. Acta 44, 943–961.

Etiope, G., Schoell, M., 2014. Abiotic gas: atypical, but not rare. Elements 10, 291–296.

Frank-Kamenetskii, V.A., 1964. The Nature of Structural Impurities and Inclusions in Minerals [in Russian]. LGU Press, Leningrad.

Futergendler, S.I., Frank-Kamenetskii, V.A., 1960. Oriented inclusions of olivine, garnet andchrome-spinel in diamond. Zapisky RMO, No. 90, 230–236.

Futergendler, S.I., Frank-Kamenetskii, V., 1964. On epitaxial character of some inclusions in diamonds. Rentgenografiya mineralnogo syr'ya, No. 4, 97–107.

Galimov, E.M., 1984. Variations of isotopic composition of diamonds and their relation with diamond formation. Geokhimiya, No. 8, 1091–1177.

Griffin, W.L., Ryan, C.G., Gurney, J.J., Sobolev, N.V., Win, T.T., 1991. Chromite macrocrysts in kimberlites and lamproites; geochemistry and origin, in: Proc. of the Fifth Intern. Kimberlite Conf., Brazil, Vol. 1, pp. 366–387.

Griffin, W.L., Sobolev, N.V., Ryan, C.G., Pokhilenko, N.P., Win, T.T., Yefimova, E.S., 1993. Trace elements in garnets and chromite: diamond formation in the Siberian lithosphere. Lithos 29, 235–256.

Grigor'ev, D.P., 1961. Ontogeny of Minerals. Lvov Univers. Public., Lvov.

Hall, A.E., Smith, C.B., 1984. Lamproite diamonds – are they different? In: Glover, J.E., Harris, P.G. (Eds.), Kimberlite occurrence and origin University of Western Australia, Geology Dept., Publ. 8, pp. 167–212.

Harris, J.W., 1968. The recognition of diamond inclusions. Part I: Syngenetic inclusions. Industr. Diam. Review, 28, 402–410.

Hartman, H., 1954. A discussion on "Oriented olivine inclusions in diamond". Am. Mineral. 39, 674–675.

Howarth, G.H., Sobolev, N.V., Pernet-Fisher, J.F., Ketcham, R.A., Maisano, J.A., Pokhilenko, L.N., Taylor, D., Taylor, L.A., 2015. 3-D X-ray tomography of diamondiferous mantle eclogite xenoliths, Siberia: A review. J. Asian Earth Sci. 101, 39–67.

Hwang, S.L., Shen, P., Yui, T.F., Chu, H.T., Logvinova, A.M., Sobolev, N.V., 2018. Low-energy phase boundary pairs and preferred crystallographic orientations of olivines in nanometer-sized ultrapotassic fluid inclusions of Aykhal diamond. Lithos 322, 392–404.

Ilupin, I.P., Efimova, E.S., Sobolev, N.V., Usova L.V., Savrasov, D.I., Khar'kiv, A.D., 1982. Inclusions in a diamond from diamondiferous dunite. Dokl. Akad. Nauk SSSR 264, 454–456.

Ireland, T.R., Rudnick, R.L., Spetsius, Z.V., 1994. Trace elements in diamond inclusions from eclogites reveal link to Archean granites. Earth Planet. Sci. Lett. 128, 199–213.

Jean, M.M., Taylor, L.A., Howarth, G.H., Peslier, A.H., Fedele, L., Bodnar, R.J., Guan, Y., Doucet, L.S., Ionov, D.A., Logvinova, A.M., Golovin, A.V., Sobolev, N.V., 2016. Olivine inclusions in Siberian diamonds and mantle xenoliths: Contrasting water and trace-element contents. Lithos 265, 31–41.

Kinny, P.D., Griffin, B.J., Heaman, L.M., Brakhfogel, F.F., Spetsius, Z.V., 1997. Shrimp U-Pb ages of perovskite from Yakutian

kimberlites. Geologiya i Geofizika (Russian Geology and Geophysics) 38 (1), 91–99 (97–105).

Kjarsgaard, B.A., Januszczak, N., Stiefenhofer, J., 2019. Diamond exploration and resource evaluation of kimberlites. Elements 15, 411–416.

Lemmlein, G.G., 1973. Morphology and Genesis of Crystals. Nauka, Moscow.

Liu, Y., Taylor, L.A., Sarbadhikari, A.B., Valley, J.W., Ushikubo, T., Spicuzza, M.J., Kita, N., Ketcham, R.A., Carlson, W., Shatsky, V., Sobolev, N.V., 2009. Metasomatic origin of diamonds in the world's largest diamondiferous eclogite. Lithos 112, 1014–1024.

Logvinova, A.M., Taylor, L.A., Floss, C., Sobolev, N.V., 2005. Geochemistry of multiple diamond inclusions of harzburgitic garnets as examined in-situ. Int. Geol. Rev. 47 (12), 1223–1233.

Logvinova, A.M., Wirth, R., Fedorova, E.N., Sobolev, N.V., 2008. Nanometre-sized mineral and fluid inclusions in cloudy Siberian diamonds: new insights on diamond formation. Eur. J. Mineral. 20 (3), 317–331.

Logvinova, A.M., Wirth, R., Tomilenko, A.A., Afanas'ev, V.P., Sobolev, N.V., 2011. The phase composition of crystal-fluid nanoinclusions in alluvial diamonds in the northeastern Siberian Platform. Russian Geology and Geophysics (Geologiya i Geofizika) 52 (11), 1286–1297 (1634–1648).

Logvinova, A.M., Taylor, L.A., Fedorova, E.N., Yelisseyev, A.P., Wirth, R., Howarth, G., Reutsky, V.N., Sobolev, N.V., 2015 A unique diamondiferous peridotite xenolith from the Udachnaya kimberlite pipe, Yakutia: role of subduction in diamond formation. Russian Geology and Geophysics (Geologiya i Geofizika) 56 (1–2), 306–320 (397–415).

McCollom, T.M., 2013. Laboratory simulation of abiotic hydrocarbon formation in Earth's deep subsurface. Rev. Mineral. Geochem. 75, 467–494.

Meyer, H.O.A., Boyd, F.R., 1972. Composition and origin of crystalline inclusions in natural diamonds. Geochim. Cosmochim. Acta 36, 1255–1273.

Meyer, H.O.A., 1987. Inclusions in diamond, in: Nixon, P.Y. (Ed.), Mantle Xenoliths. Wiley, London, pp. 501–523.

Mikhail, S., McCubbin, F.M., Jenner, F.E., Shirey, S.B., Rumble, D., Bowden, R., 2019. Diamondites: evidence for a distinct tectonothermal diamond-forming event beneath the Kaapvaal craton. Contrib. Mineral. Petrol. 174, 1–15.

Milani, S., Nestola, F., Angel, R.J., Nimis, P., Harris, J.W., 2016. Crystallographic orientations of olivine inclusions in diamonds. Lithos 265, 312–316.

Misra, K.C., Anand, M., Taylor, L.A., Sobolev, N.V., 2004. Multistage metasomatism of diamondiferous eclogite xenoliths from the Udachnaya kimberlite pipe, Yakutia, Siberia. Contrib. Mineral. Petrol. 146 (6), 696–714.

Mitchell, R.S., Giardini, A.A., 1953. Oriented olivine inclusions in diamond. Am. Mineral. 38, 136–138.

Nestola, F., Nimis P., Ziberna, L., Longo, M., Marzoli, A., Harris, J.W., Manghnani, M., Fedorchouk Y., 2011. First crystal-structure determination of olivine in diamond; composition and implications for provenance in the Earth's mantle. Earth Planet. Sci. Lett., 249–255.

Nestola, F., Nimis, P., Angel, R.J., Milani, S., Bruno, M., Prencipe, M., Harris, J.W., 2014. Olivine with diamond-imposed morphology included in diamonds. Syngenesis or protogenesis? Int. Geol. Rev. 56 (13), 1658–1667.

Nestola, F., Zaffiro, G., Mazzucchelli, M.L., Nimis, P., Andreozzi, G.B., Periotto, B., Princivalle, F., Lenaz, D., Secco, L., Pasqualetto, L., Logvinova, A.M., Sobolev, N.V., Lorenzetti, A., Harris, J.W., 2019. Diamond-inclusion system recording old deep lithosphere conditions at Udachnaya (Siberia). Sci. Rep. 9, Article 12586.

Neuser, R.-D., Schertl, H.-P., Logvinova, A.M., Sobolev, N.V., 2015. An EBSD study of olivine inclusions in Siberian diamonds: evidence for syngenetic growth? Russian Geology and Geophysics (Geologiya i Geofizika) 56 (1–2), 321–329 (416–425).

Nikolenko, E.I., Logvinova, A.M., Izokh, A.E., Afanas'ev, V.P., Oleynikov, O.B., Biller, A.Y., 2018. Cr-spinel assemblage from the Upper Triassic gritstones of the northeastern Siberian Platform. Russian Geology and Geophysics (Geologiya i Geofizika) 59 (10), 1348–1364 (1680–1701).

Nimis, P., Alvaro, M., Nestola, F., Angel, R.J, Marquardt, K., Rustioni, G., Harris, J.W, Marone, F., 2016. First evidence of hydrous silicic fluid films around solid inclusions in gem-quality diamonds. Lithos 260, 384–389.

Nimis, P., Angel, R.J., Alvaro, M., Nestola, F., Harris, J.W., Casati, N., Marone, F., 2019. Crystallographic orientations of magnesiochromite inclusions in diamonds: what do they tell us? Contrib. Mineral. Petrol, 174, Article 29.

O'Neill, H.St.C., Wall, V.J., 1987. The olivine-spinel oxyden geobarometer, the nickel precipitation curve and the oxygen fugacity of the upper mantle. J. Petrol. 28, 1169–1192.

Okrugin, A.V., Borisenko, A.S., Zhuravlev, A.I., Travin, A.V., 2018. Mineralogical, geochemical and age characteristics of the rocks of the Inagli dunite–clinopyroxenite–shonkinite massif with platinum–chromite and Cr-diopside mineralization (Aldan shield). Russian Geology and Geophysics (Geologiya i Geofizika) 59 (10), 1301–1317 (1623–1642).

Orlov, Y.L., 1959. Syngenetic and epogenetic inclusions in diamond crystals, in: Proc. Mineralog. Museum of Akad. Sci. USSR, Iss. 10, pp. 103–120.

Orlov, Y.L., 1977. The Mineralogy of the Diamond. John Wiley and Sons, New York.

Palyanov, Y.N., Khokhryakov, A.F., Borzdov, Y.M., Doroshev, A.M., Tomilenko, A.A., Sobolev N.V., 1994. Inclusions in a synthetic diamond. Dokl. Akad. Nauk SSSR, 338 (1), 78–80.

Pearson, D.G., Boyd, F.R., Haggerty, S.E., Pasteris, J.D., Field, S.W., Nixon, P.H., Pokhilenko, N.P., 1994. The characterization and origin of graphite in cratonic lithospheric mantle: a petrological carbon isotope and Raman spectroscopy study. Contrib. Mineral. Petrol. 115, 449–466.

Pernet-Fisher, J.F., Barry, P.H., Day, J.M.D., Pearson, D.G., Woodland, S., Agashev, A.M., Pokhilenko, L.N., Pokhilenko, N.P., 2019. Heterogeneous kimberlite metasomatism revealed from a combined He-Os isotope study of Siberian megacrystalline dunite xenoliths. Geochim. Cosmochim. Acta 266, 220–236.

Prinz, M., Manson, D.V., Hlava, P.F., Keil, K., 1975. Inclusions in diamonds. Garnet lherzolite and eclogite assemblages. Phys. Chem. Earth 9, 797–815.

Reutsky, V.N., Logvinova, A.M., Sobolev, N.V., 1999. Carbon isotopic composition of polycrystalline diamond aggregates with chrome inclusions from Mir kimberlite pipe, Yakutia. Geochem. Int. 37, 1073–1078.

Rodionov, A.S., Sobolev, N.V., 1985. A new find of a xenolith of graphite-bearing harzburgite in kimberlite. Soviet Geology and Geophysics (Geologiya i Geofizika), 26 (12), 32–37 (26–31).

Schmitt, A.K., Zack, T., Kooijman, E., Logvinova, A.M., Sobolev, N.V., 2019. U-Pb ages of rare rutile inclusions in diamond indicate entrapment synchronous with kimberlite formation. Lithos 350–351, Article 105251.

Sephton, M.A., Hazen, R.M., 2013. On the origins of deep hydrocarbons. Rev. Miner. Geochem. 75, 449–465.

Seroytkin, Y.V., Skvortsova, V.L., Logvinova, A.M., Sobolev, N.V., 2017. Results of study of crustallographic orientation of olivine and diamond from Udachnaya kimberlite pipe, Yakutia. Dokl. Earth Sci. 476 (2), 1155–1158.

Shatsky, V.S., Zedgenizov, D.A., Ragozin, A.L., 2016. Evidence for a subduction component in the diamond-bearing mantle of the Siberian craton. Russian Geology and Geophysics (Geologiya i Geofizika) 57 (1) 111–126 (143–162).

Shimizu, N., Sobolev, N.V., 1995. Young peridotitic diamonds from the Mir kimberlite pipe. Nature 375 (6530), 394–397.

Shirey, S.B., Cartigny, P., Frost, D.J., Keshav, S., Nestola, F., Nimis, P., Pearson, D.G., Sobolev, N.V., Walter, M.J., 2013. Diamonds and the geology of mantle carbon. Rev. Mineral. Geochem. 75, 355–421.

Sobolev, E.V., 1989. Harder Than Diamond. Nauka, Novosibirsk.

Sobolev, E.V., Lenskaya, S.V., 1965. "Gaseous" admixutes manifestations in spetrs of natural diamonds. Soviet Geology and Geophysics 6 (2), 157–159.

Sobolev, E.V., Lenskaya, S.V., Lisoyvan, V.I., Samsonenko N.D., Sobolev, V.S., 1966. Some physical properties of diamonds from Yakutian eclogite. Dokl. Akad. Nauk SSSR 168 (5), 1151–1153.

Sobolev, N.V., Lavrent'ev, Y.G., Pospelova, L.N., Sobolev, E.V., 1969a. Chrome pyropes from Yakutian diamonds. Dokl. Akad. Nauk SSSR 189 (1), 162–165.

Sobolev, N.V., 1977. Deep-Seated Inclusions in Kimberlites and the Problem of the Composition of the Upper Mantle. AGU, Washington.

Sobolev, N.V., Bartoshinskii, Z.V., Yefimova, E.S., Lavrent'ev, Yu.G., Pospelova, L.N., 1970. Olivine-garnet-chrome diopside assemblage from Yakutian diamond. Dokl. Akad. Nauk SSSR 192, 1349–1352.

Sobolev, N.V., Botkunov, A.I., Bakumenko, I.T., Sobolev, V.S., 1972. Crystalline inclusions with octahedral facies in diamonds. Dokl. Akad. Nauk SSSR 204 (1), 192–195.

Sobolev, N.V., Galimov, E.M., Ivanovskaya, I.N., Yefimova, E.S., 1979. Isotopic composition of carbon from diamonds containing inclusions. Dokl. Akad. Nauk SSSR 249 (5), 1217–1220.

Sobolev, N.V., Pokhilenko, N.P., Efimova, E.S., 1984. Diamond-bearing peridotite xenoliths in kimberlites and the problem of the origin of diamonds. Geologiya i Geofizika (Soviet Geology and Geophysics) 25 (12), 63–80 (62–77).

Sobolev, N.V., Sobolev, A.V., Pokhilenko, N.P., Yefimova, E.S., 1989. Chrome spinels coexisting with Yakutian diamonds, in: Boyd, F.R., Meyer, H.O.A., Sobolev, N.V. (Eds.), Workshop on diamonds 28th Intern. Geol. Congr., Washington D.C., pp. 105–108.

Sobolev, N.V., Kaminsky, F.V., Griffin, W.L., Yefimova, E.S., Win, T.T., Ryan, C.G., Botkunov, A.F., 1997. Mineral inclusions in diamonds from the Sputnik kimberlite pipe, Yakutia. Lithos 39 (3/4), 135–157.

Sobolev, N.V., Snyder, G.A., Taylor, L.A., Keller, R.A., Yefimova, E.S., Sobolev, V.N., Shimizu, N., 1998a. Extreme chemical diversity in the Mantle during eclogitic diamond formation: evidence from 35 garnet and 5 pyroxene inclusions in a single diamond. Int. Geol. Rev. 40 (7), 567–578.

Sobolev, N.V., Taylor, L.A., Zuev, V.M., Bezborodov, S.M., Snyder, G.A., Sobolev, V.N., Yefimova, E.S.,1998b. The specific features of eclogitic paragenesis of diamonds from Mir and Udachnaya kimberlite pipes (Yakutia). Geologiya i Geofizika (Russian Geology and Geophysics) 39 (12), 1667–1678 (653–1663).

Sobolev, N.V., Sobolev, V.N., Snyder, G.A., Yefimova, E.S., Taylor, L.A., 1999. Significance of eclogitic and related parageneses of natural diamonds. Int. Geol. Rev. 41 (2), 129–140.

Sobolev, N.V., Logvinova, A.M., Zedgenizov, D.A., Pokhilenko, N.P., Kuzmin, D.V., Sobolev, A.V., 2008. Olivine inclusions in Siberian diamonds: high-precision approach to minor elements. Eur. J. Mineral. 20 (3), 305–315.

Sobolev, N.V., Logvinova, A.M., Efimova, E.S., 2009a. Syngenetic phlogopite inclusions in kimberlite-hosted diamonds: implications for role of volatiles in diamond formation. Russian Geology and Geophysics (Geologiya i Geofizika), 50 (12), 1234–1248 (1588–1606).

Sobolev, N.V., Logvinova, A.M., Zedgenizov, D.A., Pokhilenko, N.P., Malygina, E.V., Kuzmin, D.V., Sobolev, A.V., 2009b. Petrogenetic significance of minor elements in olivines from diamonds and peridotite xenoliths from kimberlites of Yakutia. Lithos 112S, 701–713.

Sobolev, N.V., Sobolev, A.V., Tomilenko, A.A., Kuz'min, D.V., Grakhanov, S.A., Batanova, V.G., Logvinova, A.M., Bul'bak, T.A., Kostrovitskii, S.I., Yakovlev, D.A., Fedorova, E.N., Anastasenko, G.F., Nikolenko, E.I., Tolstov, A.V., Reutskii, V.N., 2018. Prospects of search for diamondiferous kimberlites in the northeastern Siberian Platform. Russian Geology and Geophysics (Geologiya i Geofizika) 59 (10), 1365–1379 (1701–1719).

Sobolev, N.V., Logvinova, A.M., Tomilenko, A.A., Wirth, R., Bul'bak, T.A., Luk'yanova, L.I., Fedorova, E.N., Reutsky, V.N., Efimova, E.S., 2019a. Mineral and fluid inclusions in diamonds from the Urals placers, Russia: Evidence for solid molecular N_2 and hydrocarbons in fluid inclusions. Geochim. Cosmochim. Acta 266, 197–219.

Sobolev, N.V., Tomilenko, A.A., Bul'bak, T.A., Logvinova, A.M., 2019b. Composition of hydrocarbons in diamonds, garnet, and olivine from diamondiferous peridotites from the Udachnaya pipe in Yakutia, Russia. Engineering 5, 471–478.

Sobolev, N.V., Yefimova, E.S., 2000. Composition and petrogenesis of Ti-oxides associated with diamonds. Int. Geol. Rev. 42 (8), 758–767.

Sobolev, V.S., 1936. Petrology of traps of the Siberian Platform, in: Proc. of Arctic Institute, Vol. 43, p. 230.

Sobolev, V.S., 1960. Formation conditions of diamond deposits. Geologiya i Geofizika 1 (1), 7–22.

Sobolev, V.S., Nai, B.S., Sobolev, N.V., Lavrent'ev, Yu.G. Pospelova, L.N., 1969b. Xenoliths of diamondiferous pyrope serpentinites from the Aikhal pipe. Dokl. Akad. Nauk SSSR 188 (5), 1141–1143.

Sobolev, V.S., Sobolev, N.V., Lavrent'ev, Yu.G., 1972. Inclusions in diamond from diamondiferous eclogite. Dokl. Akad. Nauk SSSR 207 (1), 164–167.

Sokol, A.G., Tomilenko, A.A., Bul'bak, T.A., Logvinova, A.M., 2020. Composition of reduced mantle fluids: evidence from modeling experiments and fluid inclusions in natural diamonds. Russian Geology and Geophysics (Geologiya i Geofizika) 61 (5–6), (810–865).

Stachel, T., Aulbach, S., Brey, G.P., Harris, J.W., Leost, I., Tappert, R., Viljoen, K.S., 2004. The trace element composition of silicate inclusions in diamonds: A review. Lithos 77, 1–19.

Stachel, T., Harris, J.W., 2008. The origin of cratonic diamonds-constraints from mineral inclusions. Ore Geol. Rev. 34, 5–32.

Stepanov, A.S., Shatsky, V.S., Zedgenizov, D.A., Sobolev, N.V., 2007. Causes of variations in morphology and impurities of diamonds from the Udachnaya Pipe eclogite. Russian Geology and Geophysics (Geologiya i Geofizika) 48 (9), 758–769 (974–988).

Taylor, L.A., Snyder, G.A., Crozaz, G., Sobolev, V.N., Yefimova, E.S., Sobolev, N.V., 1996. Eclogitic inclusions in diamonds: Evidence of complex mantle processes over time. Earth Planet. Sci. Lett. 142 (3–4), 535–551.

Taylor, L.A., Keller, R.A., Snyder, G.A., Wang, W.Y., Carlson, W.D., Hauri, E.H., McCandless, T., Kim, K.R., Sobolev, N.V., Bezborodov, S.M., 2000. Diamonds and their mineral inclusions, and what they tell us: A detailed "pull-apart" of a diamondiferous eclogite. Int. Geol. Rev. 42 (11), 959–983.

Truche, L., McCollom, T.M., Martinez, I., 2020. Hydrogen and abiotic hydrocarbons: molecules that change the world. Elements 16, 13–18.

Tychkov, N.S., Yudin, D.S., Nikolenko, E.I., Malygina, E.V., Sobolev, N.V., 2018. Mesozoic lithosphere mantle of the northeastern Siberian craton (evidence from inclusions in kimberlite). Russian Geology and Geophysics (Geologiya i Geofizika) 59 (10), 1254–1270 (1564–1586).

Ugap'eva, S.S., Pavlushin, A.D., Goryainov, S.V., 2015. Typomorphic characteristics of diamond crystals with olivine inclusions from Ebelyakh placer and kimberlite bodies of Yakutian diamondiferous province. Science and Education 2 (78), 28–34.

Whitney, D.L., Evans, B.W., 2010. Abbreviations for names of rock-forming minerals. Contrib. Mineral. Petrol. 95, 185–187.

Wiggers de Vries, D.F., Drury, M.R., de Winter, D.A.M., Bulanova, G.P., Pearson, D.G., Davies, G.R., 2011.Three-dimensional cathodoluminescence imaging and electron backscatter diffraction: tools for studying the genetic nature of diamond inclusions. Contrib. Mineral. Petrol. 161, 565–579.

Wiggers de Vries, D.F, Bulanova, G.P., De Corte, K., Pearson, D.G., Craven, J.A., Davies, G.R., 2013. Micron-scale coupled isotope and nitrogen abundance variations in diamonds: Evidence for episodic diamond formation beneath the Siberian Craton. Geochim. Cosmochim. Acta 100, 176–199.

Zyuzin, N.I., 1967. On nature of orientation of garnet inclusions from Yakutian diamonds. Geologiya i Geofizika 8 (6), 126–128.